Steering and Tuning of On-Chip Optical Beams

Fuwan Gan, Wei Li, Junjie Du, Hao Li, Aimin Wu, Zheng Shen, Xi Wang, Shichang Zou*

State Key Laboratory of Functional Materials for Informatics, Shanghai Institute of Microsystem and Information Technology, Chinese Academy of Sciences, 200050 Shanghai, China, *fuwan@mail.sim.ac.cn

Abstract

We report on-chip structures based on ordered dielectric nano-particle chain which can be used to steer and tune optical beams. With different elaborately designed structures, the optical beam can transmit in a negative direction, or totally reflected beyond the normal incidence with a subwavelength nanorod chain. The mechanism of the phenomenon is believed to be due to the symmetry of resonant modes in the dielectric nanoparticles. With the low-loss feature and the ultra-compact characteristic, this structure may find applications in photonic circuits.

1. Introduction

Miniaturization of photonic elements and efficient steering of optical beams are two paramount issues required for the design of integrated photonic circuits. One of the most efficient solutions is using the subwavelength resonance effect, where the resonant wavelength is much larger than the size of resonator. Subwavelength resonant units have indeed become the basic building blocks in artificially structured electromagnetic materials. Recently, various periodic structures based on nano-particles with different subwavelength resonant properties have been drawn more and more research interest for their different functions in steering and tuning optical waves under the subwavelength scale. For instance, the localized surface plasmon resonance of noble metal particles enables guiding of the optical energy below the diffraction limit [1]. The magnetic resonance of a split ring provides an effective negative magnetic permeability [2], which, when combined with metallic rods, leads to the implementation of the negative-refractive-index materials [3, 4]. The subwavelength resonant units in metamaterials also offer an approach to achieve seemingly arbitrary effective permittivity and permeability, leading to many interesting phenomena, which, among others, include invisibility cloaking [5-7], optical illusion [8], and the photonic analog of the black hole [9-11]. By carefully tuning the resonances in multiple angular momentum channels (AMCs) [12] of nano-particles to a nearly degenerate frequency, one is able to beat the single channel limit of total scattering cross section, giving rise to a super-scattering effect [13].

To date, most subwavelength resonators were based upon metal components which have advantage of the plasmonic resonance, however, the intrinsic material loss in metal is inevitable and severely limits the applications of these metal-based subwavelength resonators.

In this paper, we present another subwavelength resonators to steer and tune the optical beams [14, 15]. Our subwavelength resonator is based on an ordered array of closely spaced dielectric nano-particles which also support subwavelength resonance in the lower AMCs. With an elaborately designed structure, the optical beams can be tuned negative sharp turn, or, total reflection/transmission. With the ultra-compact characteristic and the low-loss feature in comparison with their metallic counterpart, this structure may find applications in photonic circuits.

2. Negative Sharp turn ahead for optical beams

When an optical beam strikes on an array of dielectric nanorods, as a result, the outgoing beam can propagate in a ‘‘negative’’ direction as shown in Fig. 1(d); namely, the outgoing (transmitted) beam makes a sharp turn and lies on the same side of the normal as the incident beam. Unlike another interesting phenomenon of negative refraction [3, 4], which guides the refracted beam to travel in a negative way in another effective material, the negative directional transmitted beam studied here lies in the same medium as the incident beam after passing through a single array of nano-particles. Therefore, it may serve as an optical component for beam steering in the chip-to-chip interconnect systems and on-chip architecture.

Let us start by studying the properties of resonant states in the lowest two AMCs for a single particle. For simplicity, we consider the two-dimensional case where the field is uniform in the z direction and the H field is polarized along z. Take silicon as an example of dielectric. In the optical frequency region we are interested in, the real part of its permittivity is 12.0 and the imaginary part negligible. Figures 1(a) and 1(b) show that the magnetic (H) field pattern exhibits the isotropic symmetry at resonance in the 0th AMC, corresponding to incident wavelength λ=2362 nm, and the dipole symmetry at resonance in the 1st AMC corresponding to λ=1550 nm, for a single nanorod with radius being 255 nm.

978-1-4673-5225-3/14/$31.00

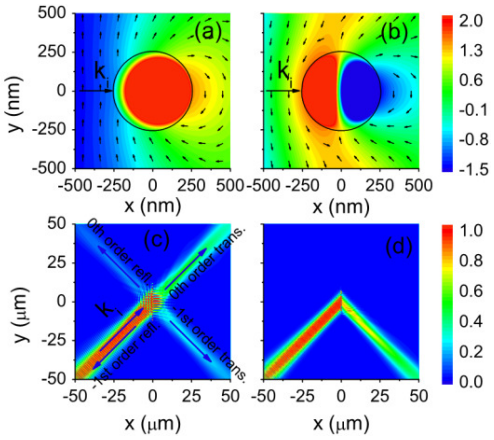

FIG. 1

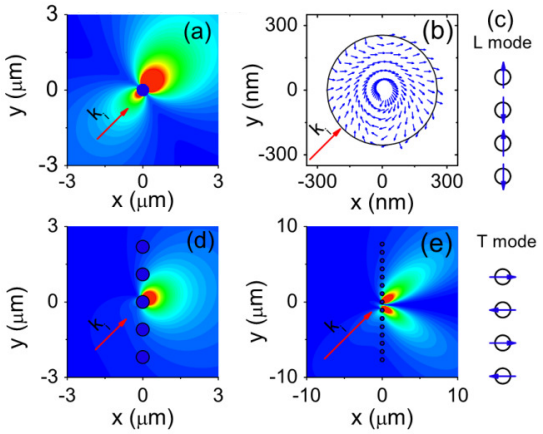

FIG. 2

FIG. 1 The field distribution at the resonance in the 0th (a) and 1st (b) AMCs, corresponding to 2362 and 1550 nm, respectively, for a single Si nanorod of radius 255 nm. The black arrows display the direction of the field on the mesh points at regular intervals outside the rod. Distribution of field intensity when a Gaussian beam strikes a single-layer array in the direction composed of 15 Si nanorods at frequencies corresponding to the resonance in the 0th (c) and 1st (d) AMCs. The arrows in (c) display the direction of four different Bragg diffracted orders.

FIG. 2. (a) The scattered H field intensity of an isolated rod at the 1st AMC resonance. (b) The time-averaged Poynting vector inside a rod located in the array, showing vortex of energy flow and implying a rotating dipole excited in the rod. (c) The longitudinal mode and transverse mode, with the excited dipole aligned along and normal to the linear array respectively. (d) The scattered H field intensity from one rod located in the array. (e) The scattered H field intensity from pair of adjacent rods in the array. The presence of many rod in (d) and (e) implies the inter-rod coupling is considered compared to the case in (a).

When the particles are arrayed in a line, the symmetry of the resonant modes of different AMCs in individual particles determines the direction of the outgoing beams. At a wavelength λ=2362 nm, corresponding to the 0th order AMC resonance, Fig. 1(c) shows that there appear four outgoing Bragg beams, in concert with the isotropic symmetry of resonant mode in the 0th AMC. For the 1st AMC resonance at a wavelength 1550 nm, the dipole symmetry completely suppresses the conventional (0th order) transmitted and reflected Bragg beams, leaving us with only one transmitted beam propagating in the negative direction, as shown in Fig. 1(d). Here the separation between adjacent rods is $a_0 = \lambda/\sqrt{2}$. Such an array functions as a grating which only supports the 0th and -1st diffraction orders when the angle of incidence is $\theta_i = 45^\circ$ [16]. The higher order reflection is usually enhanced by blazed gratings. Recently, some efforts have been made to enhance the -1st order transmission for soft-x-ray band using the total external reflection [17]. We demonstrate here that the symmetry at the 1st AMC resonance offers another way to achieve the -1st order transmission of the beam, while drastically suppressing the zeroth order reflected and transmitted waves, with the structure much thinner than the operational wavelength.

We next illustrate the correlation between the negative transmission and the dipole resonant symmetry. At the resonance in the 1st AMC, the scattered field exhibits the dipole radiation symmetry, as shown in Fig. 2(a) for a single rod. Because of this symmetry and the coupling between dipolar resonance of individual rods, the array made up of the nanorods supports two different modes: the transverse (T) mode, with dipole moments oriented perpendicular to the chain axis, and the longitudinal (L) mode, with dipole moments aligned with the chain axis [18]. The incident field excites both the and the modes but with a finite phase difference, resulting in a rotating dipole moment on each rod, which manifests itself by a finite vortex of energy flow, as shown in Fig. 2(b). The excited dipole on each rod in the array radiates in a strikingly different way from a dipole excited in an isolated rod, namely, the scattered field on the illumination side is substantially attenuated, as can be seen by a comparison between Figs. 2(a) and 2(d). This explains the vanishing of the conventional (zeroth order) reflected waves. In addition, as the incident wavelength $a_0 = \lambda/\sqrt{2}$ and incident angle $\theta_i = 45^\circ$, the induced dipole moments in adjacent rods have a phase difference of π , as schematically shown in Fig. 2(c). As a result, the scattered fields on the transmission side from a pair of adjacent rods interfere to produce radiation mainly in 0th and -1st order transmitted directions as shown in Fig. 2(e).While the scattered field in the 0th order transmitted direction cancels out the incident field, the scattered field in the -1st order transmitted direction is left as the propagating beam in negative direction, as displayed in Fig. 1(d). It is thus concluded that the phenomenon originates from the dipole symmetry of the 1st AMC resonance of the subwavelength dielectric particles.

3. Total reflection and transmission

In this section, we will discuss the total reflection or transmission phenomenon where the L and T modes are sustained by an all-dielectric subwavelength-nanorod chain. With an elaborately designed structure, both L

and T modes are excited and exhibit different effects on the near-field and far-field intensities. When a plane wave strikes on the nano-particles chain, the total reflection or transmission phenomenon in the far-field region can be seen as the destructive or constructive interference of the T mode field with the incident field.

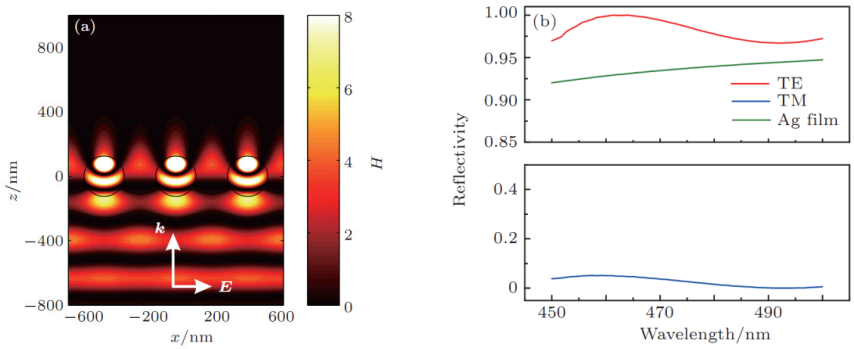

FIG.3. (a) Distribution of H field intensity when a TE mode plane wave strikes on an array of nanorods in the x direction with radius r = 125 nm. (b) Reflectivity in the blue light region.

With respect to the total reflection/transmission phenomenon, for simplicity, we consider the two-dimensional case with infinite height. An array of rods are arranged along the x direction, the separation between the adjacent particles is a0 = 445 nm. The nanorods are made of GaN, whose real part of index is about 2.5 in the blue light region, and the imaginary part is neglected. The surrounding medium is assumed to be air (n_{air} = 1). The radius of the rod is r = 125 nm. Figure 3(a) shows the magnetic (H) field intensity pattern of the transverse electric (with the H field along the y direction) mode at wavelength l = 480 nm, which is calculated by the multiple scattering theory [14, 15]. The incident wave vector is marked by the white arrow. Notice that most of the light waves towards the z direction are reflected back by the layer of nanorods. In Fig. 3(b), we present the reflectivity of the transverse electric (TE) mode in the blue light region. For comparison, the reflectivity of a typical Ag film is also presented. In practical applications, GaN-based light emitting diodes (LEDs) are widely used, however the light extraction efficiency (LEE) is not sufficiently high because of the trapping of light inside the semiconductor. One method to improve the LEE is depositing a silver film on the bottom of the LED. The reflection of the silver film results in more light being extracted from the top of the device. However, due to the metallic material absorption loss, the reflectivity of the typical Ag film is no more than 95%. With the rod array we can obtain an obviously higher reflectivity with the same semiconductor material. On the contrary, we obtain an almost opposite reflection effect for the other polarized wave, as shown in the bottom panel of Fig. 3(b). The transverse magnetic (TM) mode waves are completely separated with the TE mode waves, and the reflectivity is less than 5% from 450 nm to 500 nm. The different reflectivities for different polarized waves indicate the application for polarization suppression in light sources.

For studying the underlying physics of the total reflection or transmission phenomenon, the scattered fields of the L and T modes are presented in Fig. 4 when the chain is excited with a plane wave. The array made up of the nanorods supports two different modes: the transverse mode with the dipole moments oriented perpendicular to the chain axis, and the longitudinal mode with the dipole moments aligned with the chain axis. Figure 4(b) shows that the scattered field of the L mode is an evanescent mode and decays along the z direction, which affects the near-field distribution most, while the T mode is a propagating mode which affects the far-field distribution most, as shown in Fig. 4(c). In Fig. 4(i), the field distribution in the far-field region along x = 0 is plotted for the incident field, scattered fields of L and T modes, and the total field (composed of the scattered fields of L and T modes and the incident field). Notice that the scattered field of the L mode is almost 0 in the far-field region and the total field mainly depends on the incident field and the scattered field of the T mode. In other words, the superposition of the incident field and the scattered field of the T mode forms the total reflection phenomenon as shown in Fig. 4(d). Similarly, for another polarization, one can notice from Fig. 4(j) that the scattered field of the L mode is almost 0 in the far-field transmission region, while the field of the T mode mostly concentrates on the transmission region. A total transmission phenomenon as shown in Fig. 4(h) can be obtained as a superposition of the incident field and the scattered field of the T mode. Thus we can conclude that the total reflection or transmission phenomenon originates from the constructive or destructive interference of the T mode field with the incident wave.

4. Conclusion

To summarize, in this paper, we have shown that beam steering is possible using a single-layer array composed of high-dielectric nanorods based on the low AMC resonance. The negative sharp turn and total reflection/transmission are presented. With the capability to operate in optical frequency at low loss, the phenomenon is expected to find applications in designing compact optical components in photonic circuits

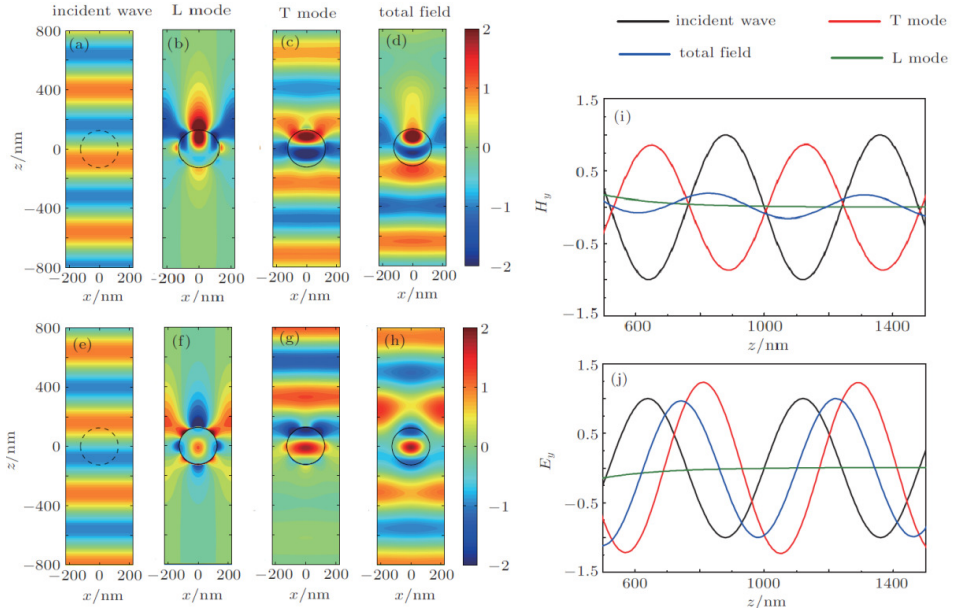

FIG.4. TE waves: (a) the contour of Hy field distribution of the incident plane wave, the scattered fields of (b) L mode and (c) T mode, (d) the total field distribution. TM waves: (e) the contour of Ey field distribution of the incident plane wave, the scattered fields of (f) L mode and (g) T mode, (h) the total field distribution. The incident field, scattered fields of T and L modes, and total field distribution along x = 0 for (i) TE wave and (j) TM wave.

5. References

1. Stefan A. Maier, Pieter G. Kik, Harry A. Atwater, Sheffer Meltzer, Elad Harel, Bruce E. Koel et al, "Local detection of electromagnetic energy transport below the diffraction limit in metal nanoparticle plasmon waveguides," *Nature Materials,* **2**, March 2003, pp.229-232.

2. J. B. Pendry, A. J. Holden, D. J. Robbins, and W. J. Stewart, "Magnetism from conductors and enhanced nonlinear phenomena," *IEEE Trans. Microwave Theory Tech.*, **47**, Nov 1999, pp. 2075-2084.

3. J. B. Pendry, "Negative Refraction Makes a Perfect Lens," *Phys. Rev. Lett.*, **85**, Oct 2000, pp. 3966-3969.

4. R. A. Shelby, D. R. Smith, S. Schultz, "Experimental Verification of a Negative Index of Refraction," *Science*, **292**, April 2001, pp. 77-79.

5. J. B. Pendry, D. Schurig, D. R. Smith, "Controlling Electromagnetic Fields," *Science*, **312**, June 2006, pp. 1780-1782.

6. U. Leonhardt, "Optical Conformal Mapping," *Science*, **312**, June 2006, pp. 1777-1780.

7. D. Schurig, J. J. Mock, B. J. Justice, S. A. Cummer, J. B. Pendry, A. F. Starr et al, "Metamaterial Electromagnetic Cloak at Microwave Frequencies," *Science*, **314**, Nov. 2006, pp. 977-980.

8. Yun Lai, Jack Ng, HuanYang Chen, DeZhuan Han, JunJun Xiao, Zhao-Qing Zhang et al, "Illusion Optics: The Optical Transformation of an Object into Another Object," *Phys. Rev. Lett.*, **102**, June 2009, 253902.

9. Dentcho A. Genov, Shuang Zhang and Xiang Zhang, "Mimicking celestial mechanics in metamaterials," *Nature Physics*, **5**, July 2009, pp. 687-692.

10. Shiyang Liu, Li Li, Zhifang Lin, H. Y. Chen, Jian Zi, and C. T. Chan, "Graded index photonic hole: Analytical and rigorous full wave solution," *Phys. Rev. B*, **82**, Aug. 2010, 054204.

11. Qiang Cheng, Tie Jun Cui, Wei Xiang Jiang and Ben Geng Cai, "An omnidirectional electromagnetic absorber made of metamaterials," *New J. Phys.*, **12**, June 2010, 063006.

12. H. C. van de Hulst, *Light Scattering by Small Particles*, Dover, New York, 1981.

13. Z. Ruan and S. Fan, "Superscattering of Light from Subwavelength Nanostructures," *Phys. Rev. Lett.*, **105**, June 2010, 013901.

14. Junjie Du, Zhifang Lin, S. T. Chui, Wanli Lu, Hao Li, Aimin Wu et al "Optical Beam Steering Based on the Symmetry of Resonant Modes of Nanoparticles," *Phys. Rev. Lett.*, **106**, May 2011, 203903.

15. Hao Li, Wei Li, Junjie Du, Aimin Wu, Chao Qiu, Zhen Sheng et al "Optical total reflection and transmission with the mode control in dielectric subwavelength nanorods chain," *Chin. Phys. B*, **22**, Nov. 2013, 117807.

16. M. Mansuripur, *Classical Optics and Its Applications* ,Cambridge University Press, Cambridge, England, 2002.

17. Ralf K. Heilmann, Minseung Ahn, Eric M. Gullikson, and Mark L. Schattenburg, "Blazed high-efficiency x-ray diffraction via transmission through arrays of nanometer-scale mirrors," *Opt. Express*, **16**, June 2008, pp. 8658-8669.

18. Alexis Devilez, Brian Stout, and Nicolas Bonod, "Mode-balancing far-field control of light localization in nanoantennas," *Phys. Rev. B*, **81**, June 2010, 245128.